

Spin and orbital magnetic state of UGe_2 under pressure

Alexander B. Shick, Václav Janiš, and Václav Drchal
Institute of Physics ASCR, Na Slovance 2, 182 21 Prague, Czech Republic

Warren E. Pickett
Department of Physics, University of California, Davis, California 95616, USA
 (Received 20 August 2003; published 18 October 2004)

The correlated band theory picture (LSDA+U) has been applied to UGe_2 , in which superconductivity has been found to coexist with robust ferromagnetism. Over a range of volumes (i.e., pressures), *two* nearly degenerate states, which differ most strikingly in their orbital character (on uranium), are obtained. The calculated moment (and its separation into spin and orbital parts) is consistent with one set of recent polarized neutron scattering data. These two states are strong candidates for the two ferromagnetic phases, one low-temperature–low-pressure, the other higher-temperature–higher pressure. Orbital (and spin) waves built from fluctuations between these uranium configurations provide a possible different mechanism of pairing in UGe_2 .

DOI: 10.1103/PhysRevB.70.134506

PACS number(s): 74.25.Jb, 74.25.Ha, 75.10.Lp

I. INTRODUCTION

The possibility of coexistence of superconductivity (SC) and ferromagnetism (FM) has long been of theoretical interest. However, the predominance of spin-singlet SC, together with the evident competition between singlet SC and FM, led to the accepted view that these two types of long-range order are mutually exclusive. Recent experiments discovered SC and FM coexistence in UGe_2 ,¹ URhGe ,² and ZrZn_2 (Ref. 3) stimulating theoretical interest in the problem. Both experiment and theory favor parallel spin pairing, magnetically mediated SC in these materials, but no microscopic material-specific theory of SC-FM coexistence exists at this time.

We focus here on the case of UGe_2 for which SC occurs in the pressure (P) range of 1.0–1.6 GPa (10–16 kBar). A very interesting feature of this material is an additional (to FM and SC ordering) phase transition (or rapid crossover), which appears as a jump in the magnetization.⁴ This magnetic moment versus pressure change has been interpreted by Sandeman, Lonzarich, and Schofield⁵ as a first-order Stoner-like phase transition in spin-only magnetization due to a sharp double-peak density of states (DOS) very near the Fermi level. We show here, using “correlated electronic structure” methods, that modest but important intra-atomic correlation effects are essential in UGe_2 . These correlations describe a change in the magnetization, but one that is associated with the change of the uranium contribution to both the orbital moment as well as the spin-magnetic moment. Our calculational results suggest an explanation of the magnetic phase transition intimately involving a change of the U orbital state in UGe_2 with pressure and temperature. The related orbital fluctuations can also provide a natural microscopic pairing mechanism, thereby tying the itinerant $5f$ electron superconductivity to the $5f$ orbital and spin magnetism.

II. COMPUTATIONAL METHOD AND RESULTS

Recent experiments on single crystals^{7,8} indicate UGe_2 to have the base-centered orthorhombic ZrGa_2 crystal structure

($Cmmm$). The structure, shown in Fig. 1, can be viewed as consisting of antiphase zigzag chains of U atoms running along the \hat{a} direction and lying within the \hat{a} - \hat{b} plane; however, interchain and intrachain U-U distances are comparable. Each U atom is tenfold coordinated by Ge. Importantly, the structure possesses inversion symmetry; without it, a FM system will not support zero-momentum Cooper pairs. Single-crystal magnetization measurements,⁶ neutron-powder diffraction measurements,⁷ and very recent single-crystal polarized neutron measurements⁸ yield a collinear magnetic structure with ferromagnetically ordered magnetic moments of 1.42–1.5 μ_B . (We quote moments per formula unit, i.e., per U atom.) The Curie temperature $T_c=52$ K at ambient pressure decreases with pressure and vanishes at

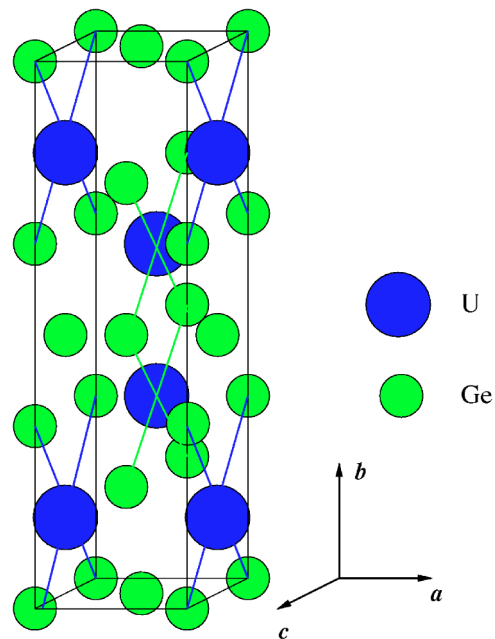


FIG. 1. (Color online) The base centered orthorhombic $Cmmm$ crystal structure of UGe_2 . The volume shown includes two primitive cells.

1.6 GPa. Around 1 GPa, Saxena *et al.*¹ and Huxley *et al.*⁹ have found that UGe₂ becomes superconducting while remaining strongly ferromagnetic (saturation magnetization $\bar{M} \approx 1 \mu_B/U$), and thereby providing the first and still the best example of coexistence of superconductivity with robust ferromagnetism.

As it was shown in Ref. 10 the conventional local spin-density (LSDA) band theory with spin-orbit coupling (SOC) included does not correctly describe the magnetic moment of 1.5 μ_B per UGe₂ formula at ambient pressure known from the experiment.¹¹ This disagreement is a consequence of the oversimplified treatment of electron correlation effects, as is often seen in the applications of LSDA to *f* electron materials. Here, we use the correlated band theory (LSDA+U) method, which consists of LSDA augmented by a correcting energy of a multiband Hubbard type and a “double-counting” subtraction term, which accounts approximately for an electron-electron interaction energy already included in LSDA. The LSDA+U method can be regarded as the static limit of the LSDA combined with the dynamical mean-field theory (LSDA+DMFT). The full-potential linearized augmented plane-wave (FP-LAPW) method including spin-orbit coupling (SOC) is used to calculate the total energy and the spin and orbital magnetic moments and their dependence on pressure, for a normal state of UGe₂ at $T=0$. When SOC is taken into account, the spin is no longer a good quantum number, and the electron-electron interaction energy E^{ee} in the LSDA+U total-energy functional¹² has to be modified. We use the generalization,¹³

$$E^{ee} = \frac{1}{2} \sum_{\gamma_1 \gamma_2 \gamma_3 \gamma_4} n_{\gamma_1 \gamma_2} (V_{\gamma_1 \gamma_3; \gamma_2 \gamma_4}^{ee} - V_{\gamma_1 \gamma_3; \gamma_4 \gamma_2}^{ee}) n_{\gamma_3 \gamma_4}, \quad (1)$$

where V^{ee} is an effective on-site Coulomb interaction, expressed in terms of Slater integrals [see Ref. 15, Eq. (3)] which are linked to intra-atomic repulsion U and exchange J . The essential feature of the generalized total energy functional Eq. (1) is that it contains spin-off-diagonal elements of the on-site occupation matrix $n_{\gamma_1 \gamma_2} \equiv n_{m_1 \sigma_1, m_2 \sigma_2}$, which become important in the presence of the large SOC.

For the given set of spin orbitals $\{\phi_{m\sigma}\}$, we then minimize the LSDA+U total energy functional. It gives the Kohn-Sham equations for a two-component spinor $\Phi_i = \begin{pmatrix} \Phi_i^\alpha \\ \Phi_i^\beta \end{pmatrix}$,¹⁴

$$\sum_{\beta} [-\nabla^2 + \hat{V}_{eff} + \xi(\vec{l} \cdot \vec{\sigma})]_{\alpha, \beta} \Phi_i^\beta(\mathbf{r}) = e_i \Phi_i^\alpha(\mathbf{r}), \quad (2)$$

where the effective potential V_{eff} is the sum of the standard (spin-diagonal) LSDA potential and on-site electron-electron interaction potential V_{+U}

$$\hat{V}_{+U}^{\alpha, \beta} = \sum_{m, m'} |\phi_{am}\rangle W^{am, \beta m'} \langle \phi_{\beta m'}|, \quad (3)$$

where

$$W^{am, \beta m'} = \sum_{p\sigma, q\sigma'} (\langle m' \beta, p\sigma | V^{ee} | m\alpha, q\sigma' \rangle - \langle m' \beta, p\sigma | V^{ee} | q\sigma', m\alpha \rangle) n_{p\sigma, q\sigma'} - \delta_{m, m'} \delta_{\beta, \alpha} [U(n - \frac{1}{2}) - J(n^\beta - \frac{1}{2})]. \quad (4)$$

The operator $|\phi_{am}\rangle \langle \phi_{\beta m'}|$ acts on the two-component spinor wave function $|\Phi\rangle$ as $|\phi_{am}\rangle \langle \phi_{\beta m'} | \Phi^\beta \rangle$. We then use the LAPW basis in the way described in Ref. 15 to solve Eq. (2) self-consistently.

We note that the LSDA contributions to the effective potential \hat{V}_{eff} in Eq. (2) (and corresponding terms in the total energy) are corrected to exclude the *f*-states nonspherical interaction. It helps to avoid the *f*-states nonspherical Coulomb and exchange energy “double counting” in LSDA and “+U” parts of the effective potential and also corrects the *f*-states nonspherical self-interaction.

Minimization of the LSDA+U total energy functional generates not only the ground state energy, but also one-electron energies and states providing the orbital contribution to the magnetic moment. The basic difference between LSDA+U calculations and the LSDA is its explicit dependence on on-site spin and orbitally resolved occupation matrices. The LSDA+U method creates, in addition to the spin-only dependent LSDA potential, the spin and orbitally dependent on-site “+U” potential, which enhances orbital polarization. The inclusion of the electron correlation-induced orbital polarization beyond that given by the LSDA (where it comes from the spin-orbit coupling only) is necessary in order to obtain the values of spin M_S and orbital M_L magnetic moments¹⁰ consistent with experiment.

We perform calculations for different values of the lattice constant a fixing the $c:b:a$ ratios and internal atomic positions as given by experiment,⁷ and we use Coulomb $U = 0.7$ eV and exchange constant $J = 0.44$ eV as in Ref. 10. In that paper it was shown that the experimentally observed total magnetic moment and the easy magnetization \hat{a} -axis direction are reproduced with these values of U and J . While $U = 0.7$ eV is somewhat smaller than might have been suspected, UGe₂ is basically an itinerant metal so this value should, in retrospect, not be so surprising. In all calculations we fix the magnetization along the \hat{a} -axis (the easy axis)¹⁰ and assume FM ordering. We used 144 special k-points in the irreducible $\frac{1}{4}$ part of the BZ, with Gaussian smearing for k-point weighting. The “muffin-tin” radius values of $R_{MT} = 3.2$ a.u. for U, and $R_{MT} = 2.0$ a.u. for Ge, and $R_{MT}^{Ge} \times K_{max} = 6.5$ (where K_{max} is the cutoff for LAPW basis set) were used. The charge and spin densities were converged better than 5×10^{-5} electron/(a.u.).³

III. TWO NEARLY DEGENERATE STATES

We find *two distinct self-consistent FM solutions* that can be sustained within the LSDA+U procedure; henceforth these states will be referred to as FM1 and FM2. The total energy E versus volume (expressed in terms of the lattice constant a) dependence, shown in Fig. 2, leads to the calculated equilibrium value $a = 7.48$ a.u. for both the FM1 and

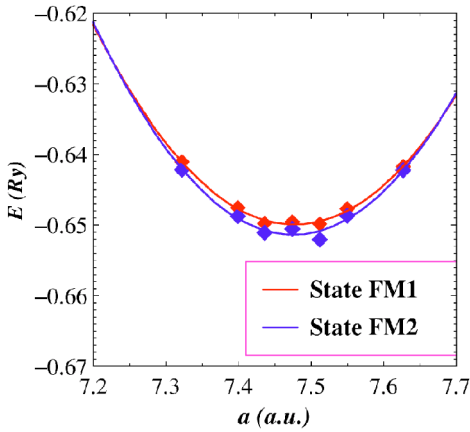


FIG. 2. (Color online) Total energy per formula unit vs lattice parameter a (see text). State FM1 is slightly higher in energy than state FM2.

FM2 states, a value that is in reasonable agreement with experimental $a=7.55-7.63$ a.u. values.^{7,8} It is noteworthy that the LSDA+U procedure used here for UGe₂ corrects about a half of the severe overbinding error in LSDA, reducing the underestimate of the volume from 9% to 4–5%. Multiple LSDA+U solutions were also found in Ce, where they seem to correspond closely to crystal field-excitation states.¹⁶

The calculated energy difference $E(\text{FM1})-E(\text{FM2}) \sim 1$ mRy/U-atom is very small and decreasing with pressure (see Fig. 2). Because of small uncertainties in the energy differences in LSDA+U calculations, we consider the FM1 and FM2 states to be essentially degenerate within the accuracy of these LSDA+U calculations. The total magnetic moment M_{tot} (per primitive cell and U atom) is comprised of the spin M_S +orbital M_L contributions. These contributions to the magnetic moment, together with the orbital moment fraction $C_2=M_L/M_{tot}$ and orbital-to-spin ratio $R_{LS}=|M_L/M_S|$, calculated at the equilibrium lattice parameter a , are given in Table I for the FM1 and FM2 states. We find good correspondence of our calculated values to the experimental values of M_{tot} and the ratios C_2 and R_{LS} ; the agreement is particularly good for the state FM2. Both our calculations and the polarized neutron scattering data⁸ clearly demonstrate the presence of a large (practically dominating) orbital magnetic moment on U atom in UGe₂. Thus both experiment and theory

TABLE I. The total magnetic moment M_{tot} (spin+orbital) per formula unit, the spin M_S , orbital M_L , and total M_{tot} magnetic moments, together with $C_2=M_L/M_{tot}$ and $R_{LS}=|M_L/M_S|$ ratios for the uranium atom, calculated at the equilibrium lattice constant a for the states FM1 and FM2.

	FM1	FM2	Expt. (Ref. 8)
M_{tot}, μ_B	1.38	1.50	1.5
M_L^U, μ_B	2.98	3.05	
M_S^U, μ_B	-1.56	-1.52	
M_{tot}^U, μ_B	1.42	1.53	1.45
$C_2=M_L^U/M_{tot}^U$	2.10	2.0	1.81
$R_{LS}= M_L^U/M_S^U $	1.91	2.0	2.24

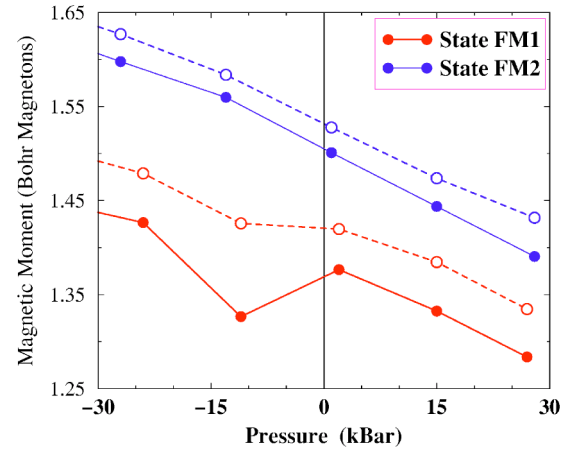


FIG. 3. (Color online) Pressure dependence of M_{tot} per primitive cell (full line) and M_{tot} per U-atom sphere (dashed line) for the states FM1 (lower pair of curves) and FM2 (upper pair).

indicate that spin-only theories of magnetic fluctuations and resulting pairing are not realistic.

We note that both LSDA+U self-consistent FM solutions persist to larger values of U . For $U=1.5$ eV, for example, these two solutions give an even better equilibrium lattice constant. However, the total magnetic moment M_S+M_L of $1.65 \mu_B$ (FM1) and $1.77 \mu_B$ (FM2) at equilibrium differs substantially from the experimental value of $1.5 \mu_B$. Since we focus mainly on the magnetic properties of UGe₂ under pressure, we use the values of U and J parameters, which provide the observed magnetization.¹⁷

We show in Fig. 3 the dependence of M_{tot} on pressure for the states FM1 and FM2. There is roughly $0.2 \mu_B$ difference in M_{tot} between these two states, which originates mainly from the U atom. Then, we can associate our results with the experimentally observed $0.5 \mu_B$ change in the magnetization under pressure [see Fig. 2(b) of Ref. 4], assuming that the sudden change in magnetization occurs as the system moves from FM2 to FM1. This is further supported energetically because the magnetic states of UGe₂ have been shown experimentally to switch in the applied field of 5T, indicating that they are extremely close in energy.

We point out that measurements of the ratio R_{LS} dependence on pressure can be a good way to probe further the origin of the magnetic states in UGe₂, since it is predicted to change rapidly from FM2 (2.0) to FM1 (1.9) in our calculations (see Fig. 4) and this ratio can be measured in polarized neutron diffraction experiments. To date only very limited experimental information on the ratios C_2 and R_{LS} is available. Kuwahara *et al.*¹⁸ reported magnetic form-factor versus pressure measurements at $P=0$ and 14 kBar and found a slight (~ 0.1) decrease of C_2 ratio with pressure (from 1.69 to 1.59 assuming U^{3+} ion configuration). From the relation $R_{LS}=C_2/(1-C_2)$, these values would lead to the orbital-to-spin ratio R_{LS} from 2.45 to 2.69. Recently, the results of Ref. 18 were complemented by measurements¹⁹ of selected magnetic peak intensities vs temperature at $P=0$ and 12 kBar. These data also indirectly suggest an increase in R_{LS} ratio (by $\sim 15\%$). Although the experimental data of Ref. 18 do not agree with our calculations, the ambient pressure C_2 and R_{LS}

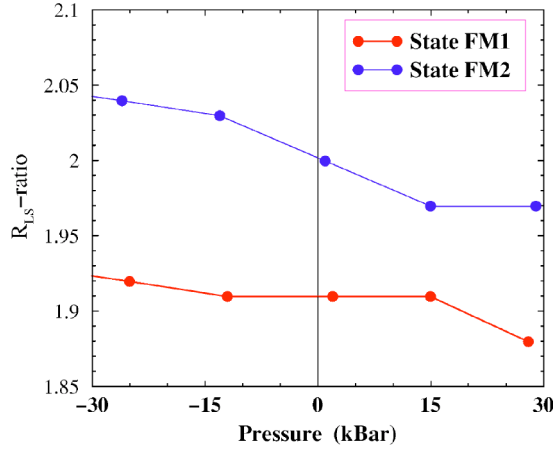


FIG. 4. (Color online) Pressure dependence of the U-atom ratio $R_{LS} = -M^l/M^s$ for state FM1 (lower curve) and FM2 (upper curve).

values which they report also differ substantially from those of Ref. 18, and accurate experimental determination of the C_2 and R_{LS} ratios under pressure with the desired accuracy (± 0.1) could be a very difficult task.

We plot in Fig. 5 the partial $5f$ DOS for the FM1 state (top) and the FM2 state (bottom) for two pressures $P = -30$ kbar and $P = 0$. The major difference between the FM1 and FM2 solutions is seen to arise from the difference between the orbital occupation of the states in the vicinity of the Fermi level: FM1 has the $|\uparrow; m_l=0\rangle$ level nearly fully

occupied, whereas FM2 has that state *unoccupied* and $|\uparrow; m_l=-1\rangle$ roughly half occupied. With increasing pressure [see Fig. 4(b)], the mixing of $|\uparrow; m_l=-1\rangle$ and $|\uparrow; m_l=0\rangle$ levels is increasing for FM2 and its electron configuration becomes closer to that of the FM1 state. This configurational instability could lead to a pronounced change in m_l at the FM2 \rightarrow FM1 transition, which would appear as a steplike change in the saturation magnetization under applied pressure.

IV. DISCUSSION AND SUMMARY

To understand the microscopic mechanism of the FM2 \rightarrow FM1 transition, we first note that it is connected with the changes in the electronic structure in the vicinity of the Fermi level E_F . It is convenient to divide the f -states into two groups according to their energy positions: “localized” $|\uparrow; m_l=-3\rangle$ and $|\uparrow; m_l=-2\rangle$, which are occupied at all volumes and, therefore, which will not contribute to the transition, and “itinerant” $|\uparrow; m_l=-1\rangle$ and $|\uparrow; m_l=0\rangle$, which straddle E_F . For simplicity, we refer them to as pure-spin- \uparrow states, while actually they also have an admixture of spin- \downarrow components due to the large SOC. We then divide the $5f$ fermionic field operator $\hat{\psi}_f = \hat{\psi}_f^{loc} + \hat{\psi}_f^{in}$ into “localized” and “itinerant” parts and write a model Hamiltonian as a sum of on-site and intersite contributions

$$\hat{H} = \sum_i \hat{H}_i^{on-site} + \sum_{i \neq j} \hat{H}_{ij}^{inter-site}. \quad (5)$$

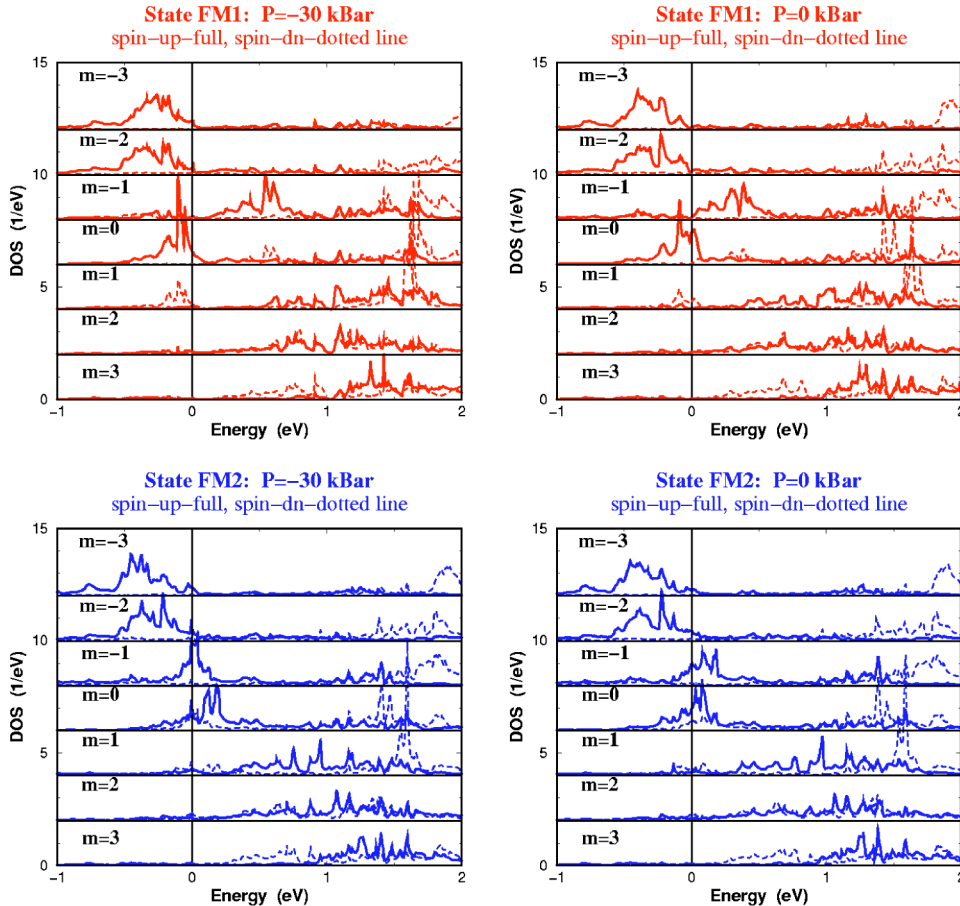


FIG. 5. (Color online) Spin and orbitally resolved U atom $5f$ DOS for the states FM1 (red) and FM2 (blue) at two different pressures.

Since the magnetic order is not changed at the FM2 \rightarrow FM1 transition, we do not expect the intersite term to contribute and will confine our attention to the on-site term only. We can further write it as an effective spin-and-orbital Hamiltonian

$$\hat{H}^i = \hat{H}^{loc}[\vec{S}_{loc}, \vec{L}_{loc}] - J\vec{S}_{loc} \cdot \vec{S}_{im} + \lambda\vec{S}_{im} \cdot \vec{L}_{im} + \frac{1}{2}\vec{L}_{im} \cdot \vec{\xi} \cdot \vec{L}_{im}. \quad (6)$$

Here, J is an effective positive intra-atomic (or Hund's) exchange coupling between localized \vec{S}_{loc} and itinerant \vec{S}_{im} spins, λ is the SOC constant, and $\vec{\xi}$ is a crystal field (CF) tensor (we assume, for simplicity, the crystal field to be quadratic due to the low-orthorhombic symmetry). Since we associate the FM2 \rightarrow FM1 transition with the change of the itinerant orbital state, only the last two terms in Eq. (6) are relevant. A further simplification can be naturally made by replacing \vec{S}_{im} and \vec{L}_{im} by single-particle \vec{s} and \vec{l} operators.

The energies then are $E(FM1) \approx E_0$ and $E(FM2) \approx E_0 - \lambda/2 + |\xi|/2$, where E_0 is a reference constant energy and $|\xi|$ is a relevant measure of the magnitude of $\vec{\xi}$. Then FM2 is lower in energy than FM1 when $\lambda > |\xi|$, otherwise the FM1 state is lower in energy.

This picture suggests that at low pressure the SOC wins over the CF energy, keeping the system in the FM2 state. With an increase of pressure, the CF increases and the FM2 \rightarrow FM1 transition occurs when the CF wins over the SOC. This scenario is quite plausible because $\lambda \sim 0.2$ eV is comparable with the usual order of magnitude of ξ for the U-based compounds. This large CF value originates from the 5*f*-states hybridization and is increasing with the increase of pressure, while the SOC scale λ remains constant.

This separation of the *f*-states into "localized" and "itinerant" follows from the results of the self-consistent calculations in which all the *f*-states are equally treated within the framework of the uniform LSDA+U electron-interaction model. This combination of characters is consistent with the unusual experimental data. The observed low-temperature magnetization¹⁹ $M(T) \sim \sqrt{1 - (T/T_c)^3}$ is somewhat intermediate between that found in the archetype *d*-metal itinerant ferromagnet Ni₃Al (Ref. 20), $M(T) \sim \sqrt{1 - (T/T_c)^2}$ and the flat Brillouin function dependence typical for local moment ferromagnets. One can also note that the spin-wave-like $M(0) - M(T) \sim T^{3/2}$ dependence is not found in UGe₂ due to a strong uniaxial MAE.

It has been suggested²¹ that superconducting *p*-wave (triplet) pairing can appear due to longitudinal magnetic fluctuations. However, that theory would also predict SC to occur in the paramagnetic regime with the transition temperature T_{SC} at least as high as in the FM-region, contradicting the experimental data (superconductivity has been observed only within the magnetically ordered regime in UGe₂, ZrZn₂, and

URhGe). To overcome the above difficulty, Kirkpatrick and coworkers²² proposed an enhancement of T_{SC} due to the magnon-to-paramagnon coupling. UGe₂ presents yet another feature: T_{SC} is maximized in the region of a transition between distinct FM phases.

An important feature of UGe₂ that has not yet been considered in models of triplet superconductors is the very large magnetocrystalline anisotropy of the FM state,^{10,23} which leads to an unusually large gap in the magnon spectrum. This characteristic of UGe₂ drives the magnons to much higher energy (they have not yet been observed) presumably making them less unlikely to drive SC pairing in this material (in addition, they are transverse magnetic excitations; see below).

Our model of FM2 \leftrightarrow FM1 local configuration fluctuations provides magnetization modulations that are candidates for the pairing "glue" for superconductivity in UGe₂. These excitations have the same longitudinal character as the magnetic excitations in the FM phase reported recently by Huxley, Raymond, and Ressouche²⁴ from neutron scattering spectra. The longitudinal aspect is essential: transverse magnetic fluctuations would be detrimental to pairing of parallel spins. Since they are comprised primarily of an intra-atomic reconfiguration of the U moment, they should have weak dispersion. It is precisely at the magnetic transition (which we identify with FM1 \leftrightarrow FM2 changes) that these configurations become degenerate, and therefore, the fluctuations become strongest. It is observed that T_{SC} is maximized at this transition. The large magnetic anisotropy is the direct result of strong spin-orbit coupling in uranium, which is also the source of the large orbital contribution to the moment (dominating over the spin part). If these modes provide the pairing, UGe₂ might best be described as driven by orbital moment fluctuations (rather than spin fluctuations).

To summarize, our LSDA+U calculations indicate the possibility for a quasi-orbitally degenerate ground state to exist in UGe₂ under pressure. The experimentally observed first-order magnetic transition is then explained by the FM2 \rightarrow FM1 change, which arises from the change of the orbital state, with both the orbital M_L and spin M_S magnetic moment components contributing to the corresponding sudden magnetization change. These findings can have an important impact on further developments of any material-specific theory for magnetically mediated SC in UGe₂.

ACKNOWLEDGMENTS

We would like to thank V. Sechovský, P. Novák, P. Oppeneer, and H. Eschrig, for discussions. One of us (A.B.S.) is grateful to A. Huxley for pointing out Ref. 18 and providing the data of Ref. 19 prior to publication. This work is supported by GACR Grant No. 202/01/0764, GAAV Grant No. Z1010914-I015, the Czech-US KONTAKT Grant No. ME-547, and NSF Grant No. DMR-0114818.

- ¹S.S. Saxena, P. Agarwal, P.K. Ahilan, F.M. Grosche, R.K.W. Haselwimmer, M.J. Steiner, E. Pugh, I.R. Walker, S.R. Julian, P. Monthoux, G.G. Lonzarich, A. Huxley, I. Sheikin, D. Braithwaite, and J. Flouquet, *Nature* (London) **406**, 587 (2000).
- ²C. Pfleiderer, M. Uhlarz, S.M. Hayden, R. Vollmer, H. von Lohneysen, N.R. Bernhoeft, and G.G. Lonzarich, *Nature* (London) **412**, 58 (2001).
- ³D. Aoki, A. Huxley, E. Ressouche, D. Braithwaite, J. Flouquet, J.P. Brison, E. Lhotel, and C. Paulsen, *Nature* (London) **413**, 613 (2001).
- ⁴C. Pfleiderer and A. Huxley, *Phys. Rev. Lett.* **89**, 147005 (2002).
- ⁵K. Sandeman, G. Lonzarich, and A. Schofield, *Phys. Rev. Lett.* **90**, 167005 (2003).
- ⁶A. Menovsky, F.R. de Boer, P.H. Frings, and J.J.M. Franse, in *High Field Magnetism* (North-Holland, Amsterdam, 1983), p. 189.
- ⁷P. Boulet, A. Daoudi, M. Potel, H. Noël, G.M. Gross, G. André, and F. Bourée, *J. Alloys Compd.* **247**, 104 (1997).
- ⁸N. Kernavanouis, B. Greiner, A. Huxley, E. Ressouche, J.P. Sanchez, and J. Flouquet, *Phys. Rev. B* **64**, 174509 (2001).
- ⁹A. Huxley, I. Sheikin, E. Ressouche, N. Kernavanouis, D. Braithwaite, R. Calemczuk, and J. Flouquet, *Phys. Rev. B* **63**, 144519 (2001).
- ¹⁰A.B. Shick, and W.E. Pickett, *Phys. Rev. Lett.* **86**, 300 (2001).
- ¹¹We note that recent LSDA results of H. Yamagami, *J. Phys.: Condens. Matter* **15**, S2271 (2003), for $M_S=1.36$ and $M_L=-2.56 \mu_B$ substantially disagree with our LSDA results¹⁰ $M_S=1.57$ and $M_L=-1.84 \mu_B$ as well as unpublished results of Yaresko and Thalmeier, $M_S=1.39$ and $M_L=-1.94 \mu_B$, which are reported in P. Thalmeier and G. Zwicky, cond-mat/0312540 (unpublished), for a reason that is unclear to us.
- ¹²V.I. Anisimov, F. Aryasetiawan, and A.I. Liechtenstein, *J. Phys.: Condens. Matter* **9**, 767 (1997).
- ¹³I.V. Solovyev, A.I. Liechtenstein, and K. Terakura, *Phys. Rev. Lett.* **80**, 5758 (1998).
- ¹⁴To simplify the notation, we use Pauli-like Hamiltonian including SOC, while the actual implementation contains in addition the scalar-relativistic terms.
- ¹⁵A.B. Shick, A.I. Liechtenstein, and W.E. Pickett, *Phys. Rev. B* **60**, 10 763 (1999).
- ¹⁶A.B. Shick, W.E. Pickett, and A.I. Liechtenstein, *J. Electron Spectrosc. Relat. Phenom.* **114–116**, 753 (2001).
- ¹⁷It is possible to obtain two FM solutions (as in fcc-Fe) in LSDA making use of a well known fixed spin moment procedure. However, a complication is that a conventional “fixed spin moment” procedure does not work when SOC is present, due to coupling of \uparrow and \downarrow spins.
- ¹⁸K. Kuwahara, H. Sagayama, K. Iwasa, M. Kphgi, Y. Haga, Y. Ōnuki, K. Kakurai, M. Nishi, K. Nakajima, N. Aso, and Y. Uwatoko, *Physica B* **312–313**, 106 (2002).
- ¹⁹A. Huxley, E. Ressouche, B. Greiner, D. Aoki, J. Flouquet, and C. Pfleiderer, *J. Phys.: Condens. Matter* **15**, S1945 (2003).
- ²⁰G. Lonzarich, *J. Magn. Magn. Mater.* **54**, 612 (1986).
- ²¹D. Fay and J. Appel, *Phys. Rev. B* **22**, 3173 (1980).
- ²²T. Kirkpatrick, D. Belitz, T. Vojta, and R. Narayanan, *Phys. Rev. Lett.* **87**, 127003 (2001).
- ²³T. Nishioka, G. Motoyama, S. Nakamura, H. Kadoya, and N.K. Sato, *Phys. Rev. Lett.* **88**, 237203 (2002).
- ²⁴A.D. Huxley, S. Raymond, and E. Ressouche, *Phys. Rev. Lett.* **91**, 207201 (2003).